Martin Storheim
Moss Maritime AS,
Vollsveien 17a,
P.O. Box 120,
Lysaker 1325, Norway
e-mail: martin.storheim@mossww.com

Hagbart S. Alsos
MARINTEK,
SINTEF Ocean,
Otto Nielsens veg 10
Trondheim 7052, Norway
e-mail: hagbart.alsos@sintef.no

Jørgen Amdahl
AMOS—Centre for Autonomous
Marine Operations and Systems,
Norwegian University of
Science and Technology,
Otto Nielsens veg 10,
Trondheim 7052, Norway
e-mail: jorgen.amdahl@ntnu.no

Evaluation of Nonlinear Material Behavior for Offshore Structures Subjected to Accidental Actions

Evaluation of the nonlinear structural response of any structure is a challenging task; a range of input parameters are needed, most of which have significant statistical variability and the evaluations require a high degree of craftsmanship. Hence, high demands are set forth both to the analyst and the body in charge of verification of the results. Recent efforts by DNVGL attempt to mitigate this with the second edition of the DNVGL-RP-C208 for the determination of nonlinear structural response, in which guidance or requirements are given on many of the challenging aspects. This paper discusses the various challenges and the direction to which the RP-C208 points compared to published research. Parameters affecting the plastic hardening, strain-rate effects, and ductile fracture are discussed separately. Then, the combined effect of the range of assumptions is evaluated to assess the resulting level of safety. [DOI: 10.1115/1.4038585]

Introduction

Design of offshore structures for infrequent actions such as collisions and wave impacts is challenging. The nature of the problem is such that it involves numerous nonlinearities and uncertainties related to material response, structural geometry, and scenario. To make the analysis even more complex, the evaluation of extreme responses is often flavored by the analysts own background and experience. In the case of evaluating the response of a collision event, the common approach goes by the use of nonlinear finite element analysis (NLFEA). Assuming that the analyst has identified the most critical and relevant accidental scenario and established a decent numerical model, the next step is to analyze the accidental response of the structure. This involves determining the plastic deformation and potential for load redistribution until the system reaches unstable failure, e.g., penetration hull, cargo tanks, or a set of compartments. The way to establish the combination of material parameters and the subsequent onset of fracture has until now been much up to the analyst and his design team to decide provided that the rationale behind the analysis is sound. With the recent update in DNVGL-RP-C208 [1], the recommendations to ductile fracture capacity and restrictions to yield level are revised. This may enhance safety with respect to design against collisions, but if not exercised with care may very well lead to unnecessary conservative accidental design.

Compared to other industries in which nonlinear response is of importance, the maritime and offshore industry does only to a very limited degree utilize material testing for calibration of the nonlinear finite element analysis simulations. Rather, the material parameters are calibrated to lower, mean, or upper bound limits to which the material batches have to be grouped. The connection between the actual material and the simulated material is thus lost. Combining this with the knowledge that the plastic response of the material is determining where and how strains will localize (and thereby where fracture will initiate, see Storheim and Amdahl [2]) raises a concern with respect to the accuracy of the simulation results. Further, when individual material parameters are assessed separately rather than combined, e.g., by minimizing the strain to failure and ultimate tensile strength separately, the resulting behavior may deviate significantly from the reality.

The material response is further complicated when fracture may occur. First, a reasonable strain localization is a prerequisite for a reasonable fracture prediction. Second, the complicated process of fracture should be included as accurately as possible, including dependencies on triaxial strain state and the different mesh effects from length-dependent strain measures to strain concentrations not captured by the adopted mesh. Inaccuracies in fracture modeling may shift the predicted response in either a conservative or a nonconservative manner, and it is not obvious if the shift is stable when changing the strain state or type of strain concentrations. Hence, a simpler method of fracture evaluation requires a significantly more conservative approach than a more refined method.

The achieved level of safety can then be discussed when combining the effects of the applied assumptions. This paper attempts to advice on the achieved level of safety and measures to improve the simulation so that the required level of safety can be reduced.

Material Strength and Plastic Hardening

Storheim and Amdahl [2] investigated the dependency on the material strength and plastic hardening for stiffened panel structures. They found that the strain localization during plastic deformation was highly dependent on the slope of the stress–strain curve; a steeper slope results in a more rapid strain localization. This is due to the mobilization of membrane force around the area with local deformation; a steep slope will rapidly mobilize a level of membrane force in the surrounding structure, whereas a less steep slope allows the strains to spread further out before the same level of membrane force is achieved.

It is vital that the assumptions used regarding the work hardening of the material are realistic as both load redistribution and fracture are a result of strain localizations. The yield ratio (yield strength to tensile strength), the elongation to tensile strength, and yield plateau all affect the slope of the stress–strain curve, and should thus be selected in consideration of the combined effect of the three parameters. As the tensile strength is more important than the initial yield strength in terms of ultimate capacity of a structure, they recommended to define the material properties by starting with tensile stress and elongation to tensile stress and then

Contributed by the Ocean, Offshore, and Arctic Engineering Division of ASME for publication in the Journal of Offshore Mechanics and Arctic Engineering. Manuscript received March 26, 2017; final manuscript received November 16, 2017; published online January 9, 2018. Assoc. Editor: Marcelo R. Martins.

Table 1 Comparison of tensile strength limits between offshore codes, low and high fractiles

	S235/NVA	S355/NV36	S420/NV42	S460/NV46
DNVGL RP-C208[a]	323–435	464–564	490–506	533–554
DNVGL OS-B101	400–520	490–630	530–680	570–720
NORSOK M-120	—	—	500–660	550–700

[a]Low fractile and mean value.

arrive at the resulting yield stress considering the yield ratio and the yield plateau. This approach will lead to realistic material behavior and can still be controlled with respect to the probability level of the material strength. The revised DNVGL-RP-C208 was developed to be more general in nature and also cover nonlinear problems in which the tensile limit is not relevant. Hence, the material curves were created from the initial yield stress rather than the tensile stress. If the same yield ratio is maintained, this approach will underestimate the tensile strength.

When evaluating the material strength of a body, it is good practice to assess whether a high or low strength is more unfavorable for the object in question. The clearest example of this is in ship collisions, where the most unfavorable combination is a high material strength of the striking vessel and a low material strength of the struck vessel. Typically, the characteristic resistance of a body should represent a 5% probability that the resistance is less than the specified value [3]. How should this be treated when two bodies interact?

Typically, we target the 10-4 annual probability of exceedance for which the load is to be calculated (kinetic energy found by use of risk analysis for a collision scenario). A low material strength of the struck vessel is a reasonable assumption, but if we at the same time assume an upper bound strength of the striking vessel it will significantly affect the total annual probability of the load. DNVGL RP-C208 opts for a lower fractile on the struck vessel and mean values for the striking vessel, which seems like a reasonable approach to obtain a combined 5% fractile of material strength without being overly conservative.

Material parameters are then defined based on the acceptance limits of the material as tested during production. Such limits are given in standards such as DNVGL OS-B101 [4] or NORSOK M-120 [5]. DNVGL-RP-C208 [1] uses EUROCODE standards [6,7] together with a limited data set from steel manufactures producing modern offshore steels to define low fractile and mean material parameters, respectively. Table 1 shows the corresponding tensile strengths from some codes and standards.

The statistical background for the material parameters in the abovementioned standards is not published. However, VanDerHorn and Wang [8] conducted a significant study on the material parameters typically used for ship construction. The data set was gathered during 2004–2009, consisting of around 140,000 tensile tests from steel mills delivering steel to ABS-classed vessels. Statistical distributions were fitted to this extensive data set, reproduced in Table 2.

The statistical distributions in Table 2 are now used to generate a new set of low fractile (5% fractile) and mean material parameters, shown in Table 3. The tensile strength values can be compared to Table 1. The lower bound tensile stress in DNVGL OS-B101 seems reasonable and is conservative, somewhat less than the 5% fractile in Table 3. The difference between the low fractile and mean value in Table 3 is fairly close due to the low coefficient of variation. Billingham et al. [9] argue that modern steels exhibit a significantly smaller statistical variance than older steels due to improved knowledge and quality control of the manufacturing process. Further, VanDerHorn and Wang [8] report that the variation between the manufacturers may be somewhat larger than that depicted in Table 2.

The values in DNVGL RP-C208 deviate significantly from the minimum requirements in DNVGL OS-B101. For high-strength steels, even the mean value in RP-C208 is below the lower bound in OS-B101.

Table 2 Statistical distribution parameters for steel material properties (from VanDerHorn and Wang [8])

Variable	Steel type	Mean	COV[a]	Distribution
Yield strength, σ_0[b]	Mild[c]	1.28	0.07	Log-normal
	HS[d]	1.18	0.06	
	HS-TM[e]	1.3	0.06	
Tensile strength, σ_{UTS}[b]	Mild	1.12	0.03	Normal[f]
	HS	1.16	0.03	
	HS-TM	1.14	0.04	
Elongation, ε[b]	Mild	1.54	0.08	Normal[f]
	HS	1.35	0.08	
	HS-TM	1.23	0.12	

[a]COV = standard deviation/mean.
[b]σ_0, σ_{UTS}, and ε represent IACS nominal rule values (as in Ref. [4]).
[c]MS: Mild steel, NVA.
[d]HS: High strength steel, AH32-EH32 and AH36-EH36.
[e]HS-TM: Thermo-mechanically rolled high strength steel.
[f]Truncated at zero.

Table 3 Material parameters calculated from Table 2

	Low fractile			Mean		
	Mild	HS	HS-TM	Mild	HS	HS-TM
Yield strength	274	385	427	301	419	461
Tensile strength	428	544	526	448	568	559
Elongation	0.31	0.26	0.22	0.34	0.28	0.26

Unfortunately, the data set in Table 2 does not say anything about the combined probability of a set of different material parameters. One such combination parameter is the yield ratio, defined as the yield stress over the tensile stress. Billingham et al. [9] and Willock [10] assessed a range of high-strength steels from which they obtained the distribution of yield ratios versus yield stress as reproduced in Fig. 1. For initial yield stresses of 355 MPa, the yield ratio ranges from 0.6 to 0.8, whereas with 460 MPa the yield ratio increases to 0.75–0.9. Thus, the relative importance of the hardening effect is smaller for high-strength steel.

Noting the importance of a realistic yield ratio in order to ensure a realistic slope of the stress–strain curve [2], the yield ratios in Fig. 1 are a vital source of information to be combined with the material parameters in Table 3 in order to ensure realistic predictions of strain concentrations. Figure 1 includes a comparison of the yield ratios from the recommended curves in

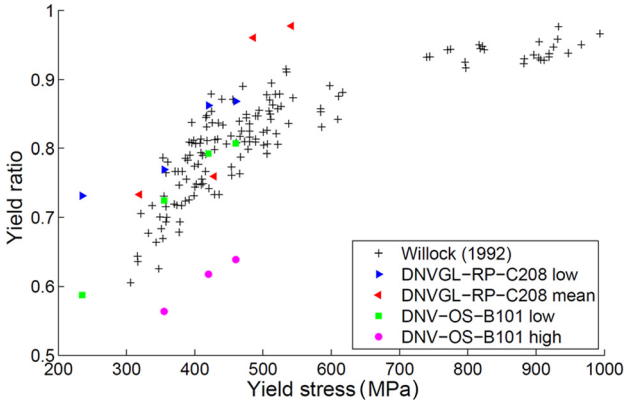

Fig. 1 Yield ratios for high-strength steels

DNVGL-RP-C208 and DNVGL-OS-B101. The low material curves in RP-C208 have yield ratios in the higher range, thus giving a conservative (low) hardening effect. However, the mean material curves are also in the high range, thereby being nonconservative when used to represent the "load" from a striking vessel by underestimating the hardening effect compared to actual materials. For S420 and S460, the RP-C208 mean values are high compared to the data in Fig. 1. This may have a significant effect on the strain localization during deformation.

Unfortunately, the elongation to fracture has not been assessed in combination with the yield ratio and tensile strength. This is an important piece of the puzzle to achieve a realistic plastic hardening from the simple material limits without doing actual material testing. An interesting challenge is that material tests are approved based on elongation to fracture and not elongation to ultimate tensile stress. The latter would be preferable as this would directly provide knowledge of the plastic work hardening, whereas models or assumptions of the postnecking behavior now have to be introduced in order to use elongation to fracture as an input parameter.

The elongation results in Table 3 thus need to be adjusted when fitting, e.g., a power law hardening model to the yield and tensile stress limits. If a too ductile material behavior is assumed, the slope of the stress–strain curve is reduced and the strain-localization will be delayed for the same tensile strength. However, if the elongation to tensile strength is assumed to be too short, the simulated material will result in too rapid strain localization and thereby premature fracture. For design purposes, it is recommended to have a realistic ductility of the material, but on the lower side of the mean value to ensure a steep enough slope of the stress–strain curve. An additional factor to keep in mind is that assuming a too low elongation to tensile strength will provoke early strain-localization by diffuse necking.

Strain-rate hardening and its effect on both the strain localization and the dynamic fracture strain is the last piece of the puzzle. Strain-rate testing is complicated experimentally, and large variations are observed between different materials. The hardening is a function of both the strain rate and the level of plastic strain (e.g., see Refs. [11] and [12]); the initial effect on dynamic yield stress is significantly larger than the effect on dynamic flow stress after finite plastic straining. Many investigators report values for the rate effect on the initial yield stress but use these data for large plastic strains, which is nonconservative as it overestimates the hardening. Storheim and Amdahl [2] showed that calibrating rate hardening to the initial yield stress may increase the structural resistance to a collision by 60%, whereas calibrating to plastic flow stress only increases the resistance by 10%. As strain-rate hardening stabilizes strain concentration, the true strain to fracture has to decrease (see Refs. [12] and [13]), even though the elongation to fracture may be constant. Further, scale effects [14] and triaxial strain-state dependence [15] have been observed in strain-rate dependent fracture occurrences.

Fracture

Fracture of stiffened panel structures is a complicated process. First, fracture itself is dependent on the strain state (triaxiality) and the deformation history of the material. Second, the process of strain localization is highly dependent on the plastic material behavior. Third, the ability to capture the correct strain concentration is highly dependent on the finite element discretization, the level of detail, and mesh refinement. Fourth, the abovementioned processes have inherent statistical variability. Fifth, the assumed load conditions will often not cover all possible scenarios, and we may thus need a contingency for such events.

When applied to new designs, the adopted methodology for fracture modeling should include the abovementioned aspects in some way and should at least cover elements 1 and 2, i.e., stress triaxiality and mesh size sensitivity. If a very simple fracture criterion is adopted (such as a constant fracture strain), it has to be combined with significant variation analyses and be subject to engineering judgment to ensure that fracture is a physical effect and represented consistently with changing structural configurations, as the criterion does not distinguish between strain states such as compression or tension. This is, however, not straightforward, and thus, to reduce the risk of design errors, the use of a well-documented criterion containing the elements identified above is recommended.

A probabilistic approach to response predictions for nonlinear accidental events would be desirable. The abovementioned aspects of fracture modeling could then be included based on a combination of predetermined quantification of, e.g., material parameters and a large number of simulations that capture the inherent variability in the most important parameters. However, this is currently not feasible due to both the lack of sufficient input data and the large computational efforts required for solving each nonlinear response scenario.

In order to evaluate how different failure criteria perform, a range of fracture criteria were investigated by Storheim et al. [16] against many different types of experiments using the nonlinear code LS-DYNA Explicit R7.0.0:

- Formability tests of mild steel as reported by Broekhuijsen [17] with strain-rate ratios β from -0.19 to 0.66 (six experiments).
- Plate-tearing tests of mild steel as reported by Simonsen and Törnqvist [18] in which a mode I-crack was driven through the plate in a controlled manner (two experiments)
- Impact tests by Alsos and Amdahl [19] in which an indenter was forced against three different panels varying stiffening (three experiments).
- Impact tests by Tautz et al. [20] in which a double-sided ship structure at scale 1:3 was deformed both by a rigid and deformable indenter (only the rigid indenter was assessed herein).
- A full-scale impact scenario with a known solution, shown in Refs. [21] and [13].

The reader is referred to the individual publications and Ref. [16] for further details of the experiments. Numerical simulations with these experiments were performed; each experiment with several different mesh sizes. Well-established fracture criteria such as the Rice–Tracey Cockroft–Latham damage criterion, Bressan-Williams-Hill (BWH) instability criterion, Germanisher Lloyds (GL) criterion, Peschmann criterion, and the constant plastic strain criterion, were evaluated. In the following, the study is extended to also include the revised RP-C208 criterion [1] and an investigation of the effect of added safety factor on the BWH criterion with postnecking damage [22].

The tested fracture criteria are described in detail in Ref. [16], except for the new criterion from DNVGL-RP-C208 [1]. This new criterion can be split into three main components:

(1) No gross yielding is allowed on a length scale of 20 times the plate thickness. For S355 steel, the maximum gross strain ε_{crg} is around 5%, measured as major principal strain. In case a high capacity is unfavorable, the gross yield criterion is to be omitted.
(2) A local membrane strain check inside the gross yield region ε_{crl} (major principal strain), where the gross failure strain is scaled as

$$\varepsilon_{crl} = \varepsilon_{crg}\left(1 + \frac{5t}{3l}\right)$$

where t is the plate thickness and l the length of the measured region (typically the element length).
(3) A local bending check, where critical strains are calibrated to a prescribed calibration case combining in-plane strain tension and out-of-plane bending.

Component 1 is based on the data collected by GL with thickness measurements of fractured plates from full-scale collision

events. However, the RP-C208 criterion deviates significantly from the GL fracture criterion [23], resulting in more than 50% reduction in dissipated strain energy to fracture with the RP-C208 criterion. No explanation is given in RP-C208 for this difference in interpretation of data. Component 3 of the criterion is not significantly different from the BWH or Rice–Tracey Cockroft–Latham criteria, but will rarely be active due to the conservative nature of components 1 and 2.

A normalized energy dissipation is defined to compare the results for the range of experiments used in the current verification study. It relates the energy dissipated in the simulation to the energy dissipated in the experiment, thereby giving a more robust scale of verification than just comparing force or displacement alone. A normalized energy of 1 means that the experiment is captured perfectly.

Two different measures were compared (illustrated in Fig. 2); the energy to peak force and the energy to end of simulation. The first represent the accuracy of the fracture criterion to predict the onset of fracture and thereby the first large drop in resistance to deformation. The latter represents the overall behavior of the complete system, including the redistribution of load in the post-fracture response. Hence, if onset of fracture is a governing design parameter, the energy to first peak force is most important. If large-scale fracture can be accepted provided that the structure does not collapse, the energy at end of simulation may be a more relevant parameter to check.

A statistical comparison of various fracture criteria was performed on the basis of a numerical study with a total of 46 simulations with around 1500 central processing unit-hours for each fracture criterion. The different experiments involve a range of materials, strain states, and types of strain localizations. Several simulations were performed for each experiment with varying mesh size. In the following, the below listed fracture criteria are evaluated:

- BWH: BWH criterion with geometric mesh scaling and coupled damage. The BWH criterion is a stress-based instability criterion that combines instability theory (local necking) with the postdamage and failure response for shell elements, as presented by Storheim et al. [22].
- BWH w. safety 1.2: BWH criterion with geometric mesh scaling and coupled damage. A safety factor of 1.2 is included in the calculation of critical principal stress for estimating onset of fracture.
- BWH w. safety 1.4: BWH criterion with geometric mesh scaling and coupled damage. A safety factor of 1.4 is included in the calculation of critical principal stress for estimating onset of fracture.
- RP-C208: The simplified criterion in RP-C208 section 5.1.3, with separate fracture strains for membrane and bending calculated according to the prescribed calibration cases. For the experimental simulations, the measured stress–strain response of the material is used, and the fracture strain evaluated based on the initial yield stress. The methodology factor of 1.2 to be used together with the criterion is disregarded.
- RP-C204: The simple criterion from DNV RP-C204 [24] (also given in NORSOK N-004) as a function of element size versus plate thickness.
- GL: The GL criterion [23], element-size dependent failure strain criterion based on measurements of fractured full-scale plates after collisions.

The variation of the safety factor of the BWH criterion is placed on the strain component which defines the BWH stress criterion. This is performed in order to visualize the effect of a potential "strain-based" safety factor. A factor directly on the stress criterion as in an "allowable stress design" is not considered as this does not combine well with plastic analyses and is therefore not considered applicable for accidental analyses.

Note that for the RP-C208 criterion, component 1 was not included in the simulations, as it would have required extensive programming efforts to evaluate the principal strain in a direction spanning over several elements. That part of the criterion is thus for postprocessing only. Further, although it is not clearly specified in DNV RP-C204 [24] or NORSOK N-004 [3], the RP-C204 criterion was intended to be evaluated over the length of the yield zone and not the element length. This may somewhat affect the predicted response of the criterion compared to the evaluations using element length herein.

Force-displacement curves from only two experiments are shown herein for brevity; the plate-tearing tests by Simonsen and Törnqvist [18] illustrate the effect of propagation of fracture and the indentation test with two flatbar stiffeners from Alsos and Amdahl [19] illustrate the onset of fracture with realistic strain concentrations in a stiffened panel structure. The force-displacement relationships for selected mesh sizes are shown in Figs. 3 and 4. Detailed results for most fracture criteria are presented in Ref. [13].

Large discrepancies can be observed from the plate-tearing results in Fig. 3, some criteria seem to capture the fracture propagation well, whereas others underestimate significantly the resistance to further fracture propagation. Similar observations can be done for the indentation experiment in Fig. 4, but some criteria overestimate the capacity due to difficulties in capturing the strain concentrations properly. The normalized energies (as defined in Fig. 2) are listed in Table 4 for both experiments for the selected fracture criteria.

The statistical properties of the normalized energies for all the simulated experiments, each with varying mesh sizes, are plotted in Fig. 5 for the different groups of tests. The total sample size is

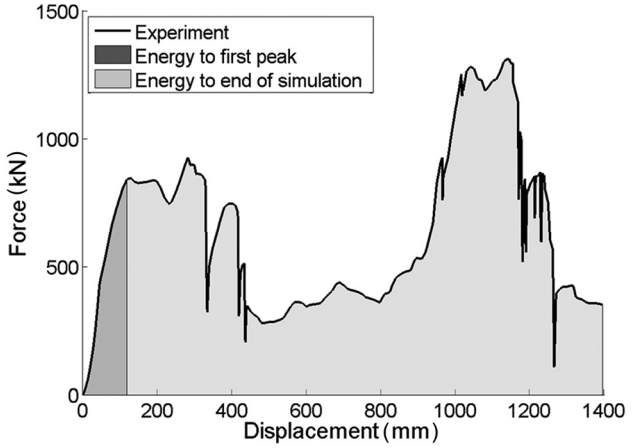

Fig. 2 Definition of normalized energy

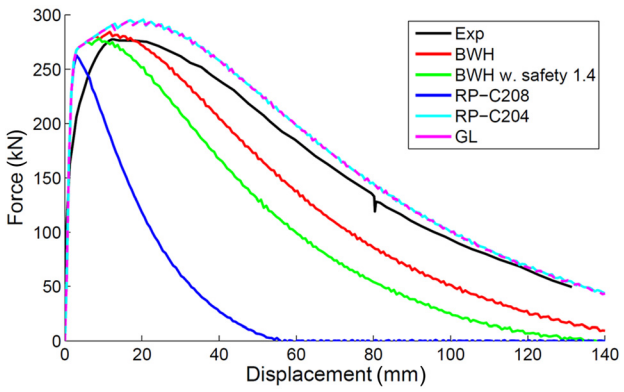

Fig. 3 Force–displacement results from simulation of the plate tearing tests from Simonsen and Törnqvist [18], 5 mm steel plate, element length equal to thickness

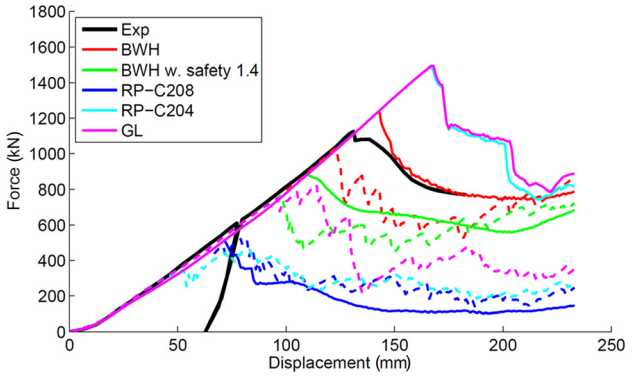

Fig. 4 Force–displacement results from simulation of the indentation experiment two flatbar stiffeners from Alsos and Amdahl [19]. Continuous lines are with element length equal to thickness, whereas dashed lines are with element length ten times the thickness.

Table 4 Normalized energies at end of experiment for the results in Figs. 3 and 4

	Simonsen and Törnqvist		Alsos and Amdahl	
	$l/t = 1$	$l/t = 8$	$l/t = 1$	$l/t = 10$
BWH	0.81	0.83	0.99	0.85
BWH w. safety 1.2	0.73	0.70	0.92	0.77
BWH w. safety 1.4	0.66	0.60	0.81	0.70
RPC208	0.24	0.33	0.34	0.43
RPC204	1.07	0.51	1.14	0.43
GL	1.07	0.66	1.14	0.66

46 simulations pr. fracture criterion; 24 material tests, four unstiffened and 18 stiffened panels. Figure 5(*a*) shows the material test results. Capturing a material test precisely is the true test of any fracture criterion; if the criterion fails to simulate the types of tests often used for calibration, it will under no circumstance be an accurate and trustworthy criterion for simulations without a known solution. The BWH criterion without safety factor shows a low statistical variation centered around about 80% of the experimental capacity. With inclusion of a safety factor, the mean decreases while the variability is fairly constant. The RP-C208 criterion systematically underestimates the experimental capacity by approximately 75%. Both the RP-C204 and the GL criterion show a large statistical variability, and the mean results overestimate the experimental capacity. A similar tendency is observed for the peak force in Fig. 5(*b*).

The simulations of the stiffened panels provide a good estimate of how the criteria behave with respect to the complex interaction between the material behavior and the structural response, complicated further by the coarse mesh discretizations. Figure 5(*c*) shows the normalized dissipated energy up to first peak force. The BWH criterion without safety factor is centered around the actual experimental capacity and with a fairly low statistical variability. Hence, the criterion gives a robust and accurate fracture prediction for onset of fracture. When including a safety factor, the capacity decreases quicker for the stiffened panels than for the material tests, likely due to the coupling between the mesh scaling and the safety factor in the BWH model. Both the RP-C204 and the GL criteria show high variability and a high mean energy to fracture.

If large-scale fracture can be accepted (provided that the residual capacity of the structure is sufficient), it is of interest to evaluate how the fracture criteria perform with respect to energy dissipation after onset of fracture. Figure 5(*d*) shows these results. Again, the BWH criterion with or without safety factors behaves consistently. On the other hand, the RP-C208 criterion reveals its conservatism, with about 50% of the energy dissipation compared to the experiments. Note that this is without consideration of component 1 of the criterion, which would further reduce the normalized energies.

Figure 5 shows that no fracture criterion is superior in all conditions. All of them may overestimate the energy dissipation in some of the test (in this respect, it is noticed that the material properties, fabrication, test setup and execution, measurements, etc., are also associated with uncertainty). The normalized energy for the GL and RPC204 fracture criteria has a mean value close to unity, but exhibits a significant variability. The RP-C208 criterion has a lower variability but tends to be very conservative. However, its coefficient of variation is large. The BWH-criterion with a safety factor of 1.2 gives a mean normalized energy of approximately 80% and a low probability of exceeding 100%. If the consequence of fracture is severe, it may be advisable to apply a safety factor directly on the strain in the BWH criterion, which was shown to perform predictably with a high accuracy in the present investigation.

Safety Factors and Combined Effects

Load resistance factor design is typically applied with ultimate limit states. For accidental limit state, most codes, including DNVGL-OS-C101 [25], specify all factors equal to unity where safety margins are placed on the material curves as indicated earlier. In general, this should be good design practice. The shortcoming of this approach is that little is said about the failure strain and the fact that the material curve can be composed in many ways. As indicated by Storheim and Amdahl [2], a steep slope on the material curve followed by a flat plateau can be overly conservative as it will lead to early stress concentrations, while a gradually increasing slope will have the opposite effect. Wrong combinations of stress curves and failure values may thus have conservative or nonconservative effects. Calibrating a fracture criterion to a specified yield curve is insufficient as the calibration will not scale properly when applied to different structural problems.

The important effect to consider when designing for accidental actions is that the safety margin reflects the failure scenario. This may either be peak force, where first fracture of the hull skin takes place, or it can be toward a certain displacement where inner compartments are penetrated. In this consideration, it is important that the safety margin through the adopted material lower, mean, or upper bound values is reflected through dissipated energy versus critical displacement or resistance. If safety margins are placed on both the material curve and failure strain, the accidental analysis may become overly conservative and will no longer correspond with the 5% fractile for exceedance. The design may become even more conservative if at the same time the slope of the material curve leads to early strain localization.

Benchmark analyses presented in the Fracture section are performed using measured stress–strain values, and the variation in safety factors placed on the BWH criterion was introduced directly on the strain component that defines the critical stress of the BWH criterion. The response of this type of "strain based" introduction of safety factors is predictable and stable, especially in scenarios where multiple failure modes occur, such as fracture and buckling. Obviously, if lower bound stresses and an unfortunate composition of the material curve were to be applied, this would lead to earlier fracture of all presented criteria. It is, thus, important that the combined effect of the composition of the material curve and failure level is carefully considered when fracture is a relevant deformation mechanism. It may not be sufficient to calibrate a simple failure strain to a simple material curve, as errors in either simple calibration can introduce new errors in the other when applied to different structural problems.

Some differences may arise between the experiments that were used in this paper to verify the structural response and the design of a full-scale structure. Some of these are related to the fact that we simulate full-scale structures during design using lower bound parameters (in some cases, severely conservative assumptions),

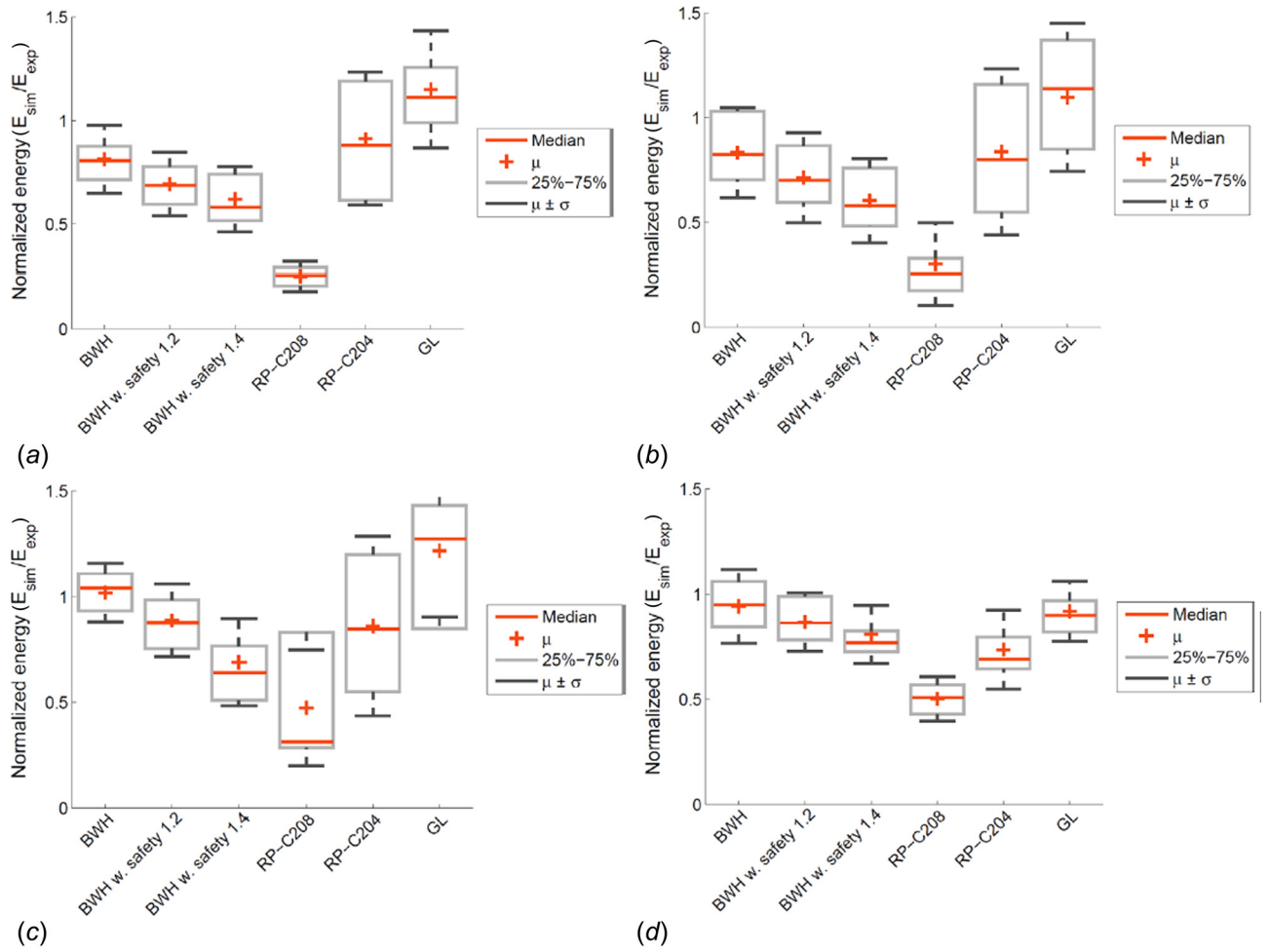

Fig. 5 Graphical view of statistical comparison of behavior of the tested fracture criteria: (*a*) material tests, peak force; (*b*) all tests, peak force; (*c*) stiffened panels, peak force; and (*d*) stiffened panels, end of simulation

which again change how the plastic strains localize and where fracture initiates. Further, there may be misalignments, bad welds, and defects in the full-scale structure that are not present in the experiments.

The proposed stress strain curves in DNVGL-RP-C208 tend to represent a lower bound in both yield stress and slope of strain hardening curve, combined with a stringent fracture limit. The degree of conservativism this implies, and whether it also should cover for other uncertainties such as early failure of undermatching welds is a matter of discussion. In the benchmark study, the RP-C208 criterion behaved very conservative, capturing less than 50% of the energy during the deformation process. Combining this with lower bound material properties, it will further reduce the level of energy, and thereby, increase the required damage to achieve the energy dissipation target. In a collision scenario in the ductile energy regime, simulations with the RP-C208 criterion would yield more than twice the damage (deformation) compared to use of the more accurate failure criteria. This may have a severe impact on the estimated ability of ships and platforms to meet the demands for robustness against accidental actions; adoption of the criterion may require significant strengthening by increasing member dimensions, material strength, structural topology, etc. It is acknowledged that the analysis of accidental actions is associated with significant uncertainties, both with respect to the intensity of the action and the structural condition, but also modeling and analysis. All things considered, we conclude that the RP-C208 criterion is unnecessarily conservative.

For scenarios in which fracture can have severe consequences, it may be appropriate to include a safety margin. This can be performed by using lower bound material data, a safety margin directly on fracture or combination of the two. Applying the safety margin on the calibration strain for the BWH criterion was shown to give predictable results. Applying a safety margin on the load (as suggested in DNVGL-RP-C208) to account for fracture will scale all deformation mechanisms equally and is generally not advisable.

Discussion and Conclusions

In the analysis and design against accidental actions, we are faced with severe challenges on how to represent material behavior with respect to initial yielding, strain hardening, ultimate strength, and fracture prediction.

As far as material parameters are concerned, the recommendation in DNVGL RP-C208 of using low fractile values for the struck ship and mean values for the striking ship seems reasonable considering the combined effect of both assumptions on the risk level. However, it may be reasonable to maintain the lower limit in DNVGL OS-B101 as a low fractile value, whereas the mean value can be estimated from Tables 2 and 3. When the material behavior is assumed to follow power law hardening with the low hardening exponents specified in DNVGL RP-C208, the resulting stress–strain relationship will deviate somewhat from the material behavior that is typically observed. This may lead to an overestimation of the strain localization in the NLFE analysis.

Recognizing the substantial uncertainties and the low level of maturity regarding the strain-rate hardening effect for coarsely meshed shell structures, it is recommended to neglect strain-rate

hardening in the simulation of relatively slow accidental actions, such as ship impacts, unless material tests are available and the rate-hardening models can be properly calibrated for the entire strain range.

Considerable work has been performed by many researches on the topic of fracture and several fracture models have been proposed, among them the new proposal in the revised DNVGL-RP-C208. Evaluations and direct comparison with tests reveal a significant spread in fracture and damage prediction between the methods. Standardization of methods for ductile fracture prediction in nonlinear finite element analysis of accidental actions is, therefore, welcomed, and guidelines for their application should help to minimize the possibility of user errors.

It is important that such guidelines are on the conservative side without being overly conservative. Based on the benchmark analyses, it is observed that the new criterion in DNVGL-RP-C208 is always on the conservative side for the reference cases. It is systematically most conservative for all the fracture criteria that were evaluated; it underestimates the energy dissipation for the benchmark tests with more than 50%. The estimated capacity will be even lower if combined with lower bound material data.

Thus, for (strain-state independent) criteria, the new RP-C208 criterion is always on the conservative side, whereas, e.g., the GL criterion may be nonconservative in certain cases. The BWH criterion provides results close to the reference cases. In combinations with safety factors or by using lower bound material data, this strain-state dependent criterion consistently produces results on the conservative side, but without being overly conservative.

Calibration of a simplified fracture criterion to an unrealistic material behavior may work for the specific calibration case, but the calibration will not transfer robustly to other structures and this procedure is generally not recommended.

The overall conclusion is that material model properties and fracture criterion specified in the new RP-C208 are unnecessarily conservative. A likely consequence of adopting this model is that structures being checked for accidental actions must be significantly strengthened to meet robustness requirements. Based on the experience from the benchmark study, we trust that material properties that give a more generous response may be used for such design purposes. The BWH criterion including postnecking damage, possibly with a strain-based safety factor, is considered to be a good candidate.

References

[1] DNVGL, 2016, "Determination of Structural Capacity by Non-Linear Finite Element Analysis Methods," DNVGL, Høvik, Norway, Report No. DNVGL RP-C208.

[2] Storheim, M., and Amdahl, J., 2015, "On the Sensitivity to Work Hardening and Strain-Rate Effects in Nonlinear FEM Analysis of Ship Collisions," J. Ships Offshore Struct., **12**(1), pp. 100–115.

[3] Standards Norway, 2004, "Design of Steel Structures," Standards Norway, Lysaker, Norway, Standard No. N-004.

[4] DNV, 2009, "Metallic Materials," DNV, Høvik, Norway, Standard No. DNV-OS-B101.

[5] Standard Norge, 2000, "Material Data Sheets for Structural Steel," Standard Norge, Lysaker, Norway, Standard No. M-120.

[6] BSI, 2008, "Execution of Steel Structures and Aluminium Structures—Part 2: Technical Requirements for Steel Structures," Brussels Studies Institute, Brussels, Belgium, Standard No. EN 1090-2:2008.

[7] BSI, 2005, "Eurocode 3: Design of Steel Structures—Part 1–2: General Rules Structural Fire Design," Brussels Studies Institute, Brussels, Belgium, Standard No. EN 1993-1-2.

[8] VanDerHorn, E., and Wang, G., 2012, "A Statistical Study on the Material Properties of Shipbuilding Steels," *Sustainable Maritime Transportation and Exploitation of Sea Resources*, Vol. 1, E. Rizzuto and C. Guedes Soares, eds., CRC Press, Boca Raton, FL, pp. 371–378.

[9] Billingham, J., Sharp, J. V., Spurrier, J., and Kilgallon, P. J., 2003, "Review of the Performance of High Strength Steels Used Offshore," Health and Safety Executive, Bedfordshire, UK, Research Report No. 105.

[10] Willock, R. T. S., 1992, "Yield: Tensile Ratio and Safety of High Strength Steels," Health and Safety Executive, Bedfordshire, UK, Research Report No. 108.

[11] Choung, J., Nam, W., and Lee, J.-Y., 2013, "Dynamic Hardening Behaviors of Various Marine Structural Steels Considering Dependencies on Strain Rate and Temperature," J. Mar. Struct., **32**, pp. 49–67.

[12] Cerik, B. C., 2016, "A Study on Modelling of Rate-Dependent Material Behaviour in Simulation of Collision Damage," 18th International Conference on Computational Geophysics and Sedimentology (ICCGS), Ulsan, South Korea, June 15–18, Paper No. ICCGS 2016-11.

[13] Storheim, M., 2016, "Structural Response in Ship-Platform and Ship-Ice Collisions," Ph.D. thesis, Norwegian University of Science and Technology, Trondheim, Norway.

[14] Jones, N., 2006, "Some Recent Developments in the Dynamic Inelastic Behavior of Structures," J. Ships Offshore Struct., **1**(1), pp. 37–44.

[15] Alves, M., and Jones, N., 1999, "Influence of Hydrostatic Stress on Failure of Axisymmetric Notched Specimens," J. Mech. Phys. Solids, **47**(3), pp. 643–667.

[16] Storheim, M., Amdahl, J., and Martens, I., 2015, "On the Accuracy of Fracture Estimation in Collision Analysis of Ship and Offshore Structures," J. Mar. Struct., **44**, pp. 254–287.

[17] Broekhuijsen, J., 2003, "Ductile Failure and Energy Absorption of y-Shaped Test Section," Master's thesis, Delft University of Technology, Delft, The Netherlands.

[18] Simonsen, B. C., and Törnqvist, R., 2004, "Experimental and Numerical Modelling of Ductile Crack Propagation in Large-Scale Shell Structures," J. Mar. Struct., **17**(1), pp. 1–27.

[19] Alsos, H. S., and Amdahl, J., 2009, "On the Resistance to Penetration of Stiffened Plates—Part I: Experiments," Int. J. Impact Eng., **36**(6), pp. 799–807.

[20] Tautz, I., Schottelndreyer, M., Lehmann, E., and Fricke, W., 2013, "Collision Tests With Rigid and Deformable Bulbous Bows Driven Against Double Hull Side Structures," Sixth International Conference on Collision and Grounding of Ships and Offshore Structures (ICCGS), Trondheim, Norway, June 17–19, pp. 93–100.

[21] Martens, I., 2014, "Konstruktive Aspekte beim Entwurf von Bugwülsten zur Verbesserung des Energieaufnahmevermögens bei Schiffskollisionen," Ph.D. thesis, Technical University of Hamburg, Hamburg, Germany.

[22] Storheim, M., Alsos, H. S., Hopperstad, O. S., and Amdahl, J., 2015, "A Damage-Based Failure Model for Coarsely Meshed Shell Structures," Int. J. Impact Eng., **83**, pp. 59–75.

[23] Scharrer, M., Zhang, L., and Egge, E. D., 2002, "Kollisions-berechnungen in schiffbaulichen entwurfssystemen (Collision Calculation in Naval Design Systems)," Germanischer Lloyd, Hamburg, Germany, Report No. ESS 2002.183.

[24] DNV, 2010, "Design Against Accidental Loads," DNV, Høvik, Norway, Report No. DNV RP-C204.

[25] DNVGL, 2014, "Design of Offshore Steel Structures, General (LRFD Method)," DNVGL, Høvik, Norway, Report No. DNV OS-C101.